Indonesian Journal of Science & Technology

Journal homepage: http://ejournal.upi.edu/index.php/ijost/

Sensitivity of Junction Width to Tidal Nonlinearity on Small and Shallow Tidal Junction

Faruq Khadami, Kiyosi Kawanisi, Mohamad Basel Al Sawaf, Gillang Noor Nugrahaning Gusti*

Department of Civil And Environmental Engineering, Graduate School Of Engineering, Hiroshima University, Japan

*Correspondence: E-mail: kiyosi@hiroshima-u.ac.jp

ABSTRACT

Observations of water elevation in the short and small tidal junctions of the Ota River, Japan, showed an increase in tidal nonlinearity at the apex of the junction. To quantitatively estimate the increase in nonlinearity, the barotropic hydrodynamic model was applied in an idealized junction domain, inspired by the Ota River Estuary junction. Even though the model was simplified, it successfully reproduced the increase in nonlinearity at the junction apex. A sensitivity analysis of tidal nonlinearity to the width of the upstream channel at the junction was performed by varying the upstream channel width from the same width as the branch channel width to three times the branch channel width. The relationship between the upstream channel width at the apex and tidal nonlinearity was not linear. Tidal nonlinearity was maximized when the apex width was twice the branch channel width. The convergence of the tides in the small width junction induced an increase of some positions of quarter-diurnal tidal constituent that raised the tidal nonlinearity. In the case of a wider channel, the flushing from river runoff dampen the tidal constituents, making it decrease tidal nonlinearity.

ARTICLE INFO

Article History:
Submitted/Received 28 May 2022
First revised 23 Jun 2022
Accepted 20 Aug 2022
First available online 22 Aug 2022
Publication date 01 Sep 2022

Keyword:
Junction width variation,
Tidal junction,
Tidal nonlinearity.

1. INTRODUCTION

Investigations of the tidal wave evolution in estuarine networks have received increasing attention in the literature. Several studies have explored the importance of the river runoff and geomorphological setting of the river to the river dynamics using various methods including remote sensing, models, and direct measurement (Amin *et al*., 2021; Arif *et al*., 2020; Pareta & Pareta, 2017).

However, many studies have been conducted in large estuarine networks such as the Yangtze (Guo *et al*., 2015) and Mahakam Rivers (Sassi *et al*., 2013), because they have high discharge and sedimentation rates.

In these estuaries, tidal wave dynamics are significantly modulated by river runoff (Guo *et al*., 2015). River runoff modulates tidal nonlinearity behavior by increasing tidal damping and asymmetry (Guo *et al*., 2015; Lu *et al*., 2015; Sassi & Hoitink, 2013).

The effect of convergence of tidal waves in a junction is much less clear. Several studies show a tidal wave convergence induces an amplification and decreases water level amplitude, such as in Buschman *et al*., (2010). Some observations show an increase in a tidal compound and over-tide tidal constituents amplitude (Sassi & Hoitink, 2013).

However, based on observation, Xiao *et al*., (2021) found that the convergence of tides in small channel show the tidal range did not significantly affect the M4 tidal constituent.

Moreover, they only focused on the junction's apex without explaining the changes in water level dynamics before and after convergence. Using numerical experiments, Buschman *et al*., (2010) show convergence of tidal waves in junction affects the division of tidal discharge in the branches.

Danial *et al*., (2019) show a similar result to Buschman *et al*., (2010) and suggest that the neap-spring tidal variation controls discharge asymmetry.

Moreover, in a tidal junction, the division of discharge and tidal convergence may strongly influence the sediment division (Xiao *et al*., 2021) and affect the morphodynamics of the channel (Iwantoro *et al*., 2020).

From those previous studies, it is clearly shown that the bifurcation geometry significantly affects the tidal wave dynamics and morphodynamics in estuaries. However, those studies focus on the variation of the asymmetrical branches and relatively little explanation of the effect of the upstream channel. As a result, the role of the upstream channel geometry is still less clear.

In a tidal-dominated estuary, where the ratio of river runoff to tidal discharge is less than one, the modulation of the river runoff to the tidal wave nonlinearity behavior is low.

The evolution of tidal waves is affected more by shallow water friction concerning bottom topography changes (Bilskie, *et al*., 2019; Khadami *et al*., 2020; MacMahan *et al*., 2014; Xiao *et al*., 2021). Using analytical approaches, the relation between friction and convergence channel in the tidal-dominated estuary was examined by Savenije *et al*. (2008).

However, this study was limited to a single, straight channel. Small estuarine networks with limited discharge have achieved poor recognition, and the variation in the topographical setting is rarely discussed.

Studies on tidal wave evolution in small and narrow estuary networks have provided a better understanding of tidal dynamics.

The water elevation in estuarine networks is more complicated than that in straight tidal rivers. In an estuarine tidal network, tides propagate from multiple tidal inlets to the estuaries.

Topographical settings, including variations in bathymetry and channel length and width, affect tidal propagation (Wagner & Mohrig, 2019).

This study focused on the water elevation in shallow and narrow tidal junctions with limited river runoff. Moreover, in estuarine tidal junctions, the tidal range drops because

DOI: https://doi.org/10.17509/ijost.v7i2
p- ISSN 2528-1410 e- ISSN 2527-8045

of the convergence of tidal propagation at the apex of the junction (Buschman *et al*., 2010).

Understanding the variables controlling tidal nonlinearity behavior is important because tides may become a dominant factor that controls sediment transport and nutrient mixing in estuarine networks. However, this study limits the studies on the sensitivity of water elevation to variations in the upstream channel width.

2. LITERATURE REVIEW

Bifurcations are common in estuaries systems where the upstream channel branches into a small downstream channel. The tide in estuaries plays a role in the circulation in bifurcation by affecting the magnitude of ebb and flow currents.

In a tidal-influenced system, the development of the branching channel is different from river dominated channel, where the channel asymmetries in tidal estuaries are smaller than in the river-dominated channel (Iwantoro *et al*., 2020).

The tidal effect partly cancels the inequality of discharge division (Buschman *et al*., 2010; Danial *et al*., 2019) that influenced the sediment flux division (Wagner & Mohrig, 2019) and channel development (Iwantoro *et al*., 2020).

Moreover, the geometrics of the channel, including depth and length, have a significant role in determining the asymmetry of discharge and sediment flux division (Buschman *et al*., 2010; Wagner & Mohrig, 2019).

The tidal wave dynamics in estuaries have been studied in a range of topography settings, from single channel estuaries (Cai *et al*., 2018; Savenije *et al*., 2008) to branching estuarine systems (Buschman *et al*., 2010; Danial *et al*., 2019; Xiao *et al*., 2021). It was found that the tidal wave dynamics in estuaries are controlled by interaction tides and river runoff and affected by the topography setting.

The setting topography includes the shape of the channel, depth, width, and length variation (Buschman *et al*., 2010; Iwantoro *et al*., 2020). Moreover, the setting of topography influenced the bed roughness and shear stress (Buschman *et al*., 2010).

The balance between the influence of the tides-river runoff interaction and shear stress determines the deformation of tidal wave amplitude in estuaries (Cai *et al*., 2018). In estuaries with branching topographical settings, the convergence of tides in a junction causes tidal wave deformation.

Using numerical model experiments, Buschman *et al*. (2010) showed that there is a significant decrease in tidal wave amplitude in the junction. Xiao *et al*. (2021) confirm the results using field observation data that shows a significant tidal deformation in the tidal junction.

Several studies examine the behavior of tidal waves and morphodynamics to the setting of the branching channel. Wagner & Mohrig (2019) hypothesizes that the variation of the downstream channel's length, width, and depth determines the location of tidal wave convergence from the branches.

Buschman *et al*. (2010) examined the variation of the setting of the downstream channel to the discharge division, and Iwantoro *et al*. (2020) examined the variation of the downstream depth to the channel development.

Most studies in branching channels examine the setting of the downstream channel to the tidal behavior while studies of the upstream channel's role in the tidal dynamics are still less clear. The studies written above are summarized in **Table 1**.

DOI: https://doi.org/10.17509/ijost.v7i2
p- ISSN 2528-1410 e- ISSN 2527-8045

Table 1. Summary of literature review.

Authors	Research Topic/Question	Methodology	Finding
Buschman *et al*. (2010)	Subtidal Flow division at a shallow tidal junction	Idealized hydrodynamic junction model	• Depth and length differences between channels enhance unequal subtidal flow division • Hydraulic roughness differences and tidal effect partly cancels the inequality in river flow division
Sassi & Hoitink (2013)	River flow controls water level profiles in tidal freshwater river	Observation of water elevation and flow velocity Decomposition of subtidal friction	• The river flow enhances friction that induces dumping of tidal amplitude. • The river flow enhanced the friction related to river-tide interaction.
Danial *et al*. (2019)	Characteristics of tidal discharge	Observation using Acoustics Tomography Systems	• Inequality of flow division is prominent during spring tide.
Wagner & Mohrig (2019)	Flow and sediment flux asymmetry in branching channel delta	Observation currents, temperature, salinity, and turbidity	• Geometric differences of the main channel and branches drive the asymmetry of sediment flux.
Iwantoro *et al*. (2020)	Morphological evolution of bifurcations in tide-influenced delta	Idealized hydrodynamic junction model with variation in depth, length, and tidal forcing	• The morphology of the downstream channels becomes less asymmetric with the increasing influence of tides over the river.
Xiao *et al*. (2021)	Mapping tidal currents and salinity using an acoustics tomography system	Observation using acoustic tomography systems	• The currents during the neap are driven by density currents • Increasing tidal wave deformation occurred with increasing tidal range shows the limited role of river flow

3. METHODS

3.1. Observation Location and Data

The Ota River Estuary is an estuarine network dominated by tidal forcing and is located in Hiroshima city, Japan. The tidal wave penetrates the estuary, reaching 13 km from the river mouth. The tidal range is up to 2-3.5 in the semi-diurnal tidal regime. The gate controls the discharge, with the normal discharge being around 20-100 m3/s (Danial *et al*., 2019; Xiao *et al*., 2020). The average bottom topography is approximately 3 m. Moreover, the Ota River is a branching delta. Thus, the river is suitable for studying tidal dynamics in the multi-channel estuary. The studied junction is located 5.3 km upstream of the river mouth (**Figure 1**). The junction involved the upstream Kyu Ota branch (northern branch), downstream Kyu Ota (west side branch), and Motoyasu (east side branch). Danial *et al*. (2019) studied the Misasa junction located 1 km upstream from the junction and showed the existence of tidal discharge asymmetry induced by branch channel geometry variation. At the same junction, Xiao *et al*. (2021) showed that limited river runoff plays a role in tidal asymmetry at the tidal junction.

DOI: https://doi.org/10.17509/ijost.v7i2
p- ISSN 2528-1410 e- ISSN 2527-8045

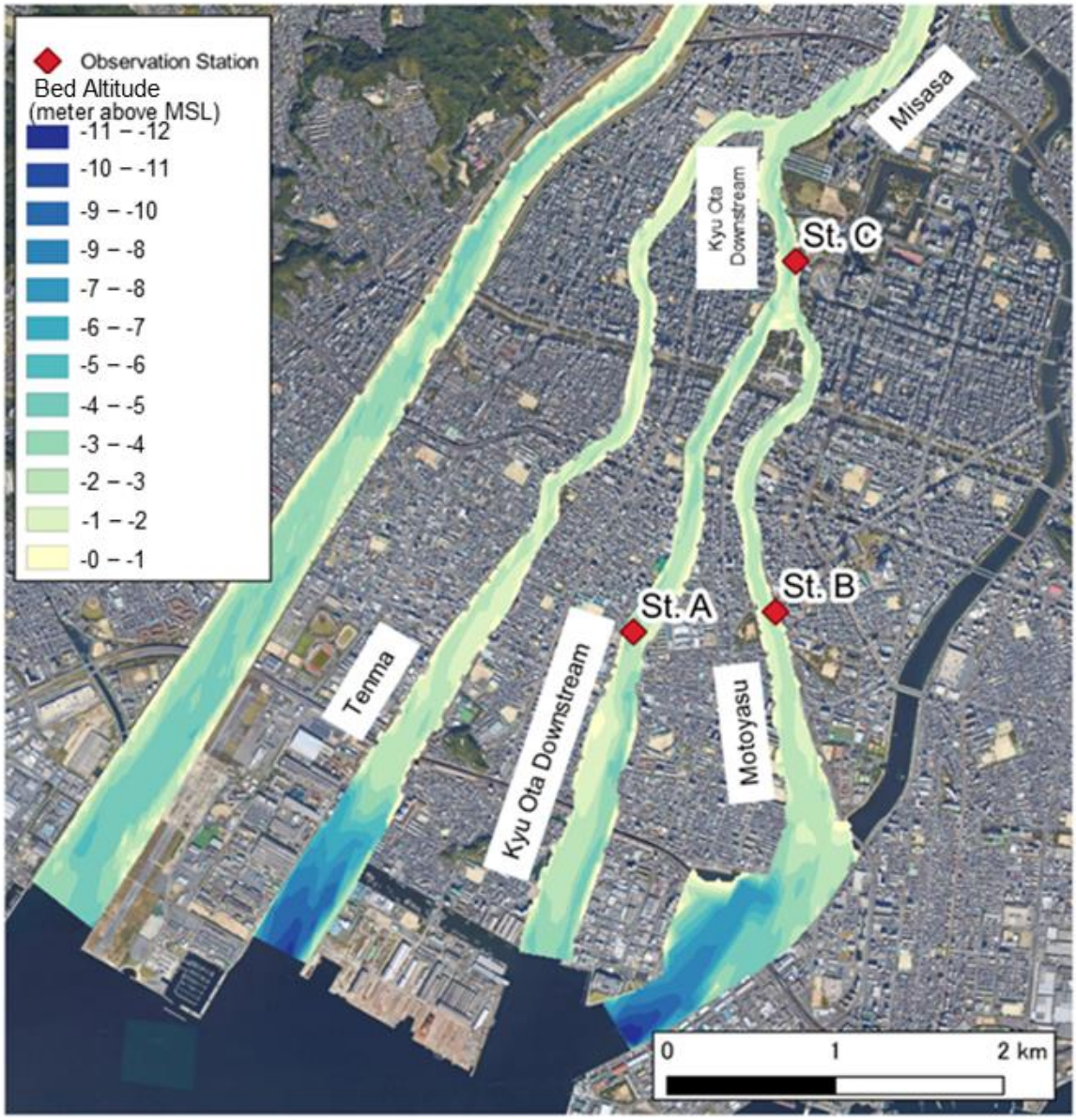

Figure 1. Ota River channel network.

The water elevation at three stations at St. A, B, and C was observed using a pressure sensor from Acoustic Doppler Current Profiler (ADCSP) during 12–30 July 2021. St. A and B were located downstream of Kyu Ota and Motoyasu branches, respectively. St. C was located at the junction upstream of the Kyu Ota branch. Observational data are shown in **Figure 2**. During the neap tide, the water elevations at St. A and St. B had the same amplitude and phase (**Figure 2a**), whereas the water elevation at St. C had slightly different amplitudes and phases (**Figure 2b**). On the other hand, during spring tide, at the highest high-water level, St. A and St. B's water elevations were higher than St. C (**Figure 2c**); however, at the second high-water level, St. C's water elevation was higher than St. B and St. A. Unfortunately, during the lowest low water level, we could not capture the water elevation data at St. C and St. A because the station was dry. Visually, this observation shows a difference in tidal asymmetry between the straight channels in the Sts. A-B and St. C. Tidal asymmetry assessment require further

DOI: https://doi.org/10.17509/ijost.v7i2
p- ISSN 2528-1410 e- ISSN 2527-8045

analysis to quantify asymmetry. Moreover, this result motivated the modeling examination, which aimed to understand the variables controlling tidal asymmetry at junctions.

3.2. Tidal Asymmetry Analysis

Harmonic analysis using the T_Tide package (Pawlowicz *et al*., 2002) was applied to the water elevation data to decompose them into tidal constituent amplitudes and phases. In this study, the water elevation data was decomposed in to semi-diurnal (M2) and quarter-diurnal (M4) tidal constituents. The method shows that the time series data are composed of summation harmonic signals with a certain frequency, amplitude, and phase, as follows Eq. (1).

$$H(t) = b_0(t) + \sum_{n=1}^{N}[A_n \cos(\omega_n t - \Phi_n)] + r(t) \quad (1)$$

where the water elevation time series is denoted as $H(t)$, $b_0$is the mean water level. A, ω, and Φ are the tidal amplitude, the frequency, and the phase, respectively, of tidal constituents *n* (*n=1,2…N*). $r(t)$ represents the residual components.

The outcome of the harmonic analysis is the amplitude and phase, which were utilized to estimate tidal asymmetry. The tidal asymmetry was calculated from the amplitude ratio of the tidal constituents (Hoitink *et al*., 2003). In this study, the ratio amplitudes of M4 and M2 were used to estimate tidal distortion because the tidal regime in the Ota River Estuary is semi-diurnal (Xiao *et al*., 2021).

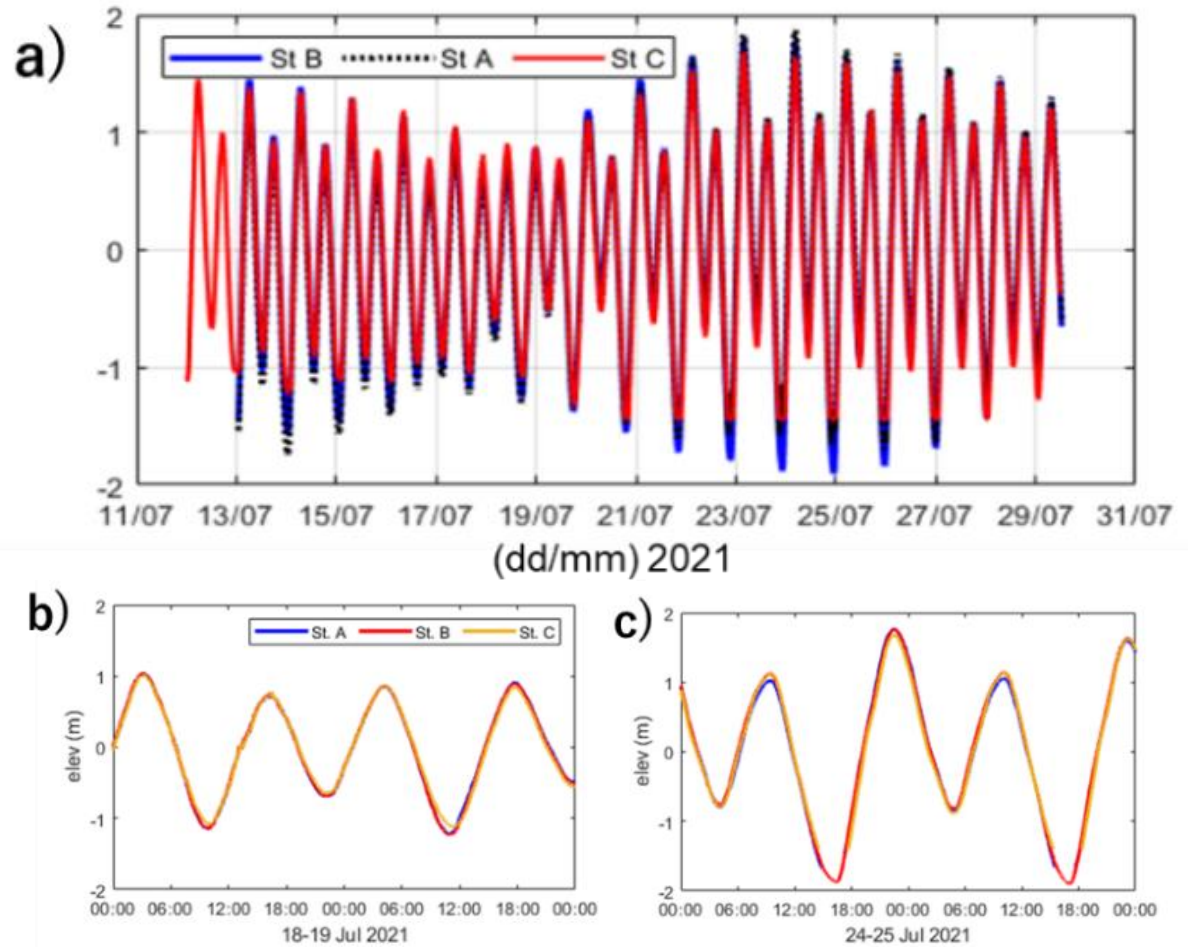

Figure 2. Water elevation observation in St. A, B, and C (a) during the observations, (b) during the neap tide, and (c) during spring tide.

DOI: https://doi.org/10.17509/ijost.v7i2
p- ISSN 2528-1410 e- ISSN 2527-8045

3.3 Numerical Experiments

A depth-averaged version of the Delft3D model is used in this study. The depth-averaged model was selected instead of a 3-dimensional model because the 3-dimensional flow is not important for studying the propagation of tidal waves. Furthermore, this model uses a barotropic mode and neglects density gradient.

An idealized model of the junction was built based on the Ota River Estuary junction. The model grid was shown in **Figure 3. Figure 3(a)** is the downstream part of the model domain, including the upstream channel and the branch that connects to the sea, whereas **Figure 3(b)** is the grid surroundings of the tidal junction.The junction was located 10 km from the open-sea boundary, and the total length of the channel was 560 km. The upstream channel was set to be very long to ensure that the tides were smoothly damped. The depth and width of the channel were designed based on the average depth and width of the Kyu-Ota junction. The upstream branch width was 160 m, and the width of the downstream branches was 70 m. In this model, tidal forcing was limited to only the M2 and S2 tidal constituents because the Ota River Estuary was dominated by semi-diurnal tides.

The parameter settings are listed in **Table 2**. Moreover, a series of simulations were conducted to analyze the sensitivity of the model to width changes, while the other parameters were fixed. The width of the upstream channel varied from 70 to 208 m. The sensitivity test aims to explain how the change in the width of the upstream branch affects the nonlinear behavior of the water elevation in the junction.

Table 2. Parameter setting of idealized junction model.

Symbol	Variable	Value
Δx	along channel grid size	40-170 m
Δy	cross channel grid size	10 m
h	still water depth	5 m
L	length of the seaward channel	10 km
Q	river discharge	50 m^3s^{-1}
M2	amplitude of M2	0.7 m
S2	amplitude of S2	0.4 m
Width Branch	width seaward branch	70 m
Width Apex	width upstream branch	160 m
C	Chezy coefficient	55 $m^{1/2}s^{-1}$

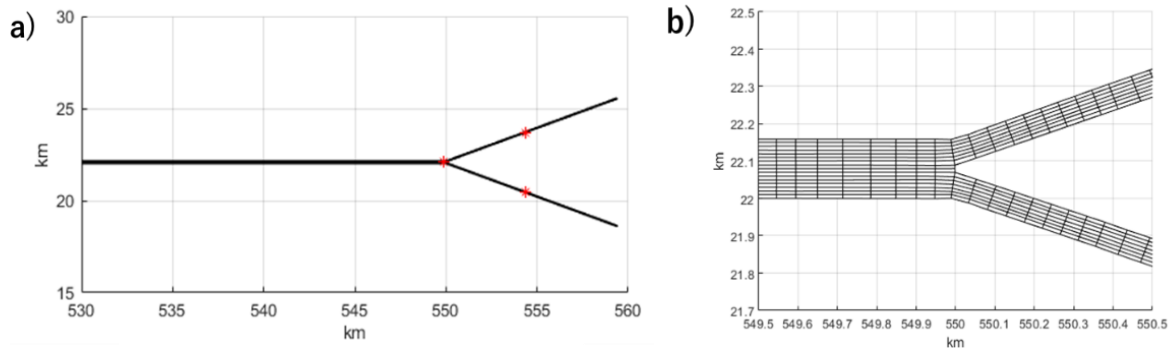

Figure 3. a) Downstream part of the model domain, including the upstream channel and the branch that connects to the sea. b) The grid surroundings of the tidal junction.

DOI: https://doi.org/10.17509/ijost.v7i2
p- ISSN 2528-1410 e- ISSN 2527-8045

4. RESULTS

4.1. Water Level Nonlinearity

Harmonic analysis on 25-hour window water elevation data showed that the amplitudes of M2 and M4 varied in the spring-neap cycle (**Figure 4**). **Figure 4** is the amplitude results. **Figures 4(a, c)** are for M2, whereas **Figures 4(b, d)** are for M4. **Figures 4(a, b)** are from observation data, whereas **Figures (c, d)** are from idealized model. The highest amplitudes of M2 and M4 occurred during the spring tide. M2 amplitudes at St. A and B were similar, whereas the M2 amplitude was lower at St. C. In contrast, the M4 amplitude at St. C was higher than those at St. A and B. Although the amplitudes M2 at St. A and B had similar values, the M4 amplitudes at St. A and B had slightly different values and peaks. The topographical setting, including the bathymetric profile, channel length, and width, could have affected the different M4 amplitude profiles at St. A and St. B. A significant increase in M4 at St. C indicates that the nonlinearity increases at the apex of the junction.

The application of harmonic analysis to the water elevation of the idealized junction model showed a pattern similar to the observations, where the amplitude of M2 at the apex of the junction was less than the M2 amplitude in the downstream branches, and the M4 amplitude at the apex of the junction was higher than the M4 amplitude in the branches. However, both the amplitude M2 and M4 models exhibit lower values than the observations. The difference between the model and the observations can be attributed to the high degree of simplification of the model. However, the model reproduced the increase in tidal nonlinearity from the downstream to the apex of the junction.

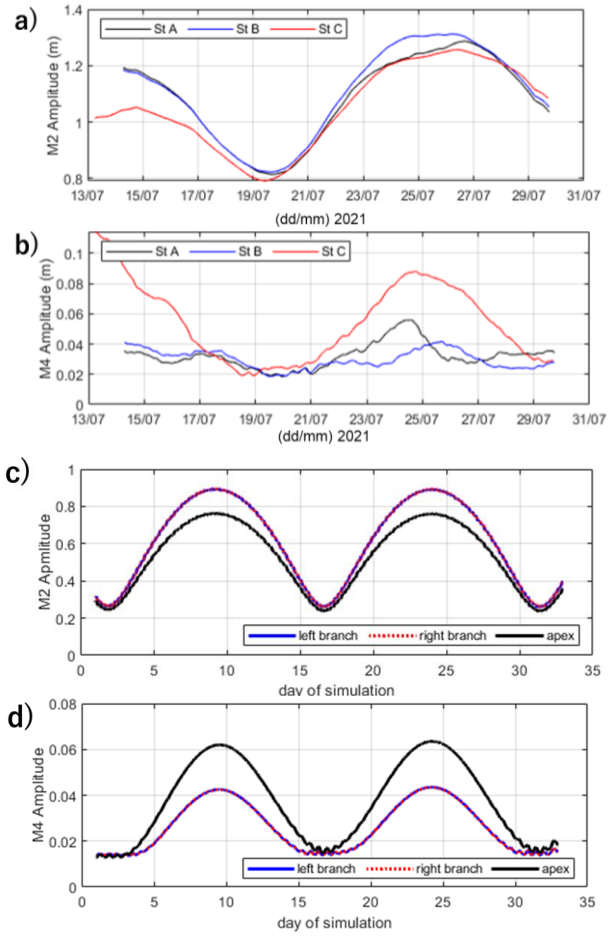

Figure 4. Amplitude results. Figures (a, c) are for M2, whereas Figures (b, d) are for M4. Figures (a, b) are from observation data, whereas Figures (c, d) are from idealized model.

DOI: https://doi.org/10.17509/ijost.v7i2
p- ISSN 2528-1410 e- ISSN 2527-8045

4.2. Sensitivity Analysis

Sensitivity analysis by varying the upstream channel width is shown in **Figure 5**. **Figures 5 (a), (b), (c),** and **(d)** are M2 left branch, M4 left branch, M2 Apex, and M4 apex, respectively. Only the amplitudes of M2 and M4 at the apex of the junction and left branch are shown because the amplitudes of M2 and M4 at the right and left branches have the same value. The results showed that the M2 amplitude at the left branch and apex decreased with an increase in upstream channel width. In contrast, the M4 amplitude showed an increasing pattern with increasing upstream channel width. However, an exception pattern was observed at the 206-m upstream channel width. The M4 amplitude was 0.07 m during the spring and 0.02m during neap, which is less than the amplitude of M4 at 160 and 112 m channel widths.

The damping/amplification of water elevation is affected by friction and the cross-sectional area of the channel changes (Savenije *et al*., 2008). Sensitivity analysis examined the changes in the cross-section of the water elevation damping/amplification by varying the width of the upstream channel. The results show that the damping of the tidal wave increased with a larger cross-sectional area. It is observed that the M2 amplitude decreases with an increase in the upstream channel width. However, this behavior was not observed for the M4 tidal constituent. In the case of M4, it increased when the width of the upstream channel was more than twice that of the downstream channel.

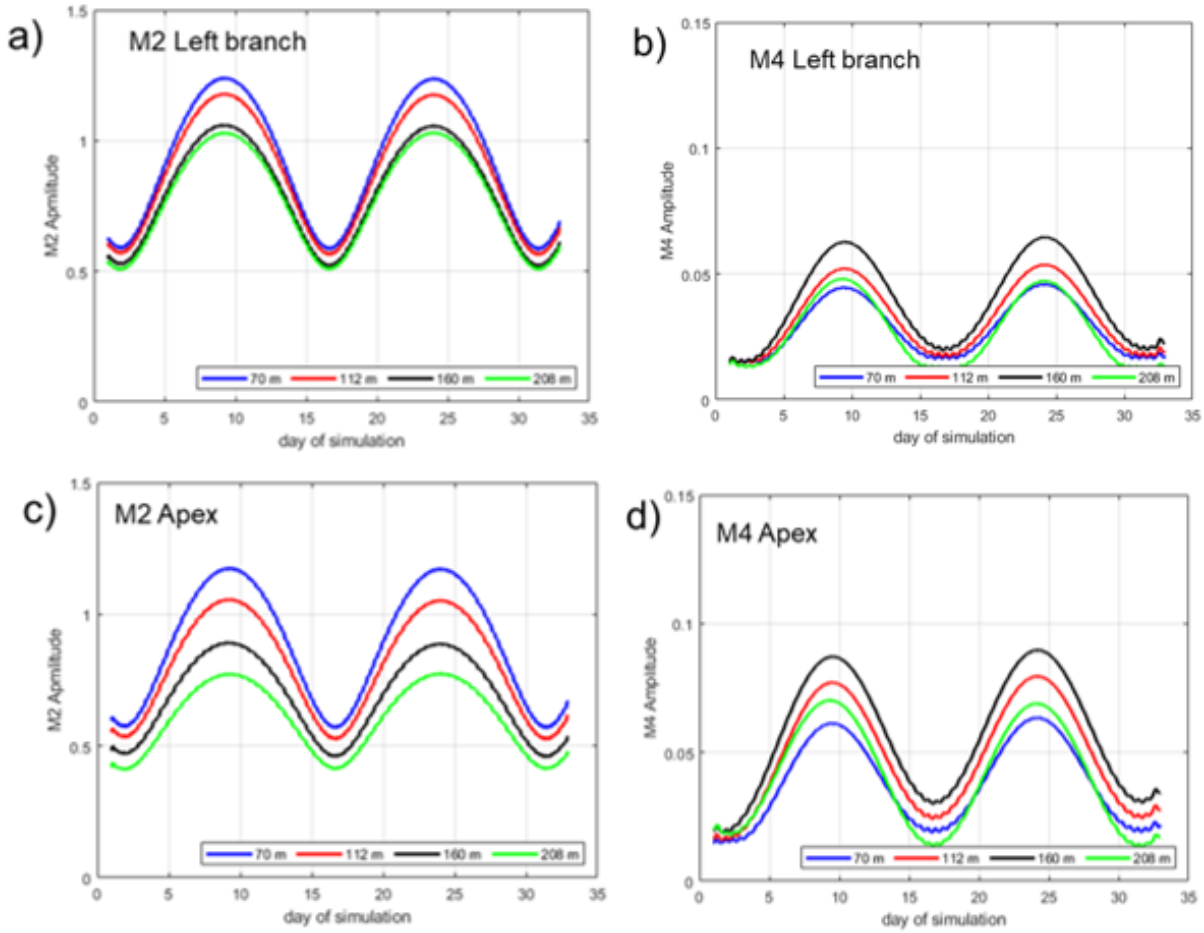

Figure 3. Amplitude of M2 and M4. Figures (a), (b), (c), and (d) are M2 left branch, M4 left branch, M2 Apex, and M4 apex, respectively.

DOI: https://doi.org/10.17509/ijost.v7i2
p- ISSN 2528-1410 e- ISSN 2527-8045

5. DISCUSSION

Figures 6 and **7** summarise the sensitivity analysis of the junction with changes in the upstream channel width. When the channel width increased, the amplitude of M2 gradually decreased. This occurs in all the time-window harmonic analyses. However, harmonic analysis of the neap tide window showed the lowest amplitude owing to low tidal forcing during the neap tide, whereas in the 30 days window harmonic analysis showed the mean value of the M2 amplitudes. In contrast, the amplitude of M4 increased with the width of the channel, except for the 220 m width of the upstream channel.

The application of the model at the junction is highly simplified. The Ota River junction is more complex with variations in geometry and bathymetry. The complexity of the junction is not considered in this model. Moreover, at the Ota River junction, the branches of the junction (downstream Kyu Ota and Motoyasu) are connected downstream. However, the simplified model can capture the nonlinear phenomena that occur at the junction.

The sensitivity of the water elevation at the junction was analyzed for one parameter at a time to identify the upstream channel width changes in tidal nonlinearity at the junction. The ratios of the M4 and M2 amplitudes were used to measure the nonlinearity (**Figure 6**). We found that nonlinearity increased as the width of the channel increased until the width of the upstream channel was twice that of the downstream channel. This result suggests that the cross-sectional area changes induced damping of the M2 tidal constituent and increased the M4 tidal constituent. When the width of the upstream channel was more than twice that of the downstream channel, nonlinearity decreased significantly. A wider cross-sectional area induced stronger damping of the M2 constituent. However, the role of river runoff flushing was more influential in a wider channel. River runoff flushing dampened the increase in M4 This process caused a decrease in nonlinearity when the width of the upstream channel was more than twice that of the downstream channel. The nonlinearity of tidal elevation was affected by the geographical setting and river discharge. A decrease in the amplitude ratio indicates an increase in river runoff (Kukulka *et al*., 2003). Horrevoets *et al*. (2004) explained that the critical point where river runoff dominated tidal damping was when the river runoff velocity was larger than the tidal velocity. River runoff velocity could be a factor that determines the maximum tidal nonlinearity. However, the study was conducted in a straight channel, and studies on tidal junctions require further research.

A decrease in the amplitude ratio in Figure 6 indicates that role of river discharge in tidal dumping increases (Kukulka & Jay, 2003; Matte *et al*., 2019). The influence of river discharge dominates the dynamics in estuaries when the river discharge more than tidal discharge (Horrevoets *et al*., 2004; Khadami *et al*., 2022; Matte *et al*., 2019). The critical number of the damping is determined by the accumulation of the effect of river discharge, estuary shape, and bottom friction (Cai *et al*., 2018). Since this sensitivity analysis variated the width upstream channel and set a uniform river discharge and estuaries shape, the effect of the upstream channel's width determines the river discharge's role in the tidal damping. When the cross-section area of the upstream channel is more than twice the cross-section area of branches, the convergent tides from the branches become minimum, and the discharge could play a significant role in dampening the tidal wave (Wu *et al*., 2022).

The finding suggests that the changes in the cross-section area of the upstream channel could significantly change the hydrodynamics pattern. Furthermore, the hydrodynamics changes will disturb the morphology stability in estuaries. Xiao *et al*.,

DOI: https://doi.org/10.17509/ijost.v7i2
p- ISSN 2528-1410 e- ISSN 2527-8045

(2021) showed a bifurcation flow phenomenon in asymmetries junctions, where the tides that come from one branch propagate to the other branch because of the asymmetrical shape of estuaries. Moreover, the asymmetrical length and depth of the channel cause the convergence of the tides is not at the apex of unction (Iwantoro *et al*., 2020; Wagner & Mohrig, 2019). Morphological instability could happen in the convergence location of tides and river discharge caused by sediment dynamics, including erosion/deposition sediment (Iwantoro *et al*., 2022; Wagner & Mohrig, 2019). Since this research limited the focus on the effect of channel width on the tidal nonlinearity, exploration of other topography settings on the tidal nonlinearity, such as channel depth length, as well as asymmetrical estuaries shape, need to conduct in further research.

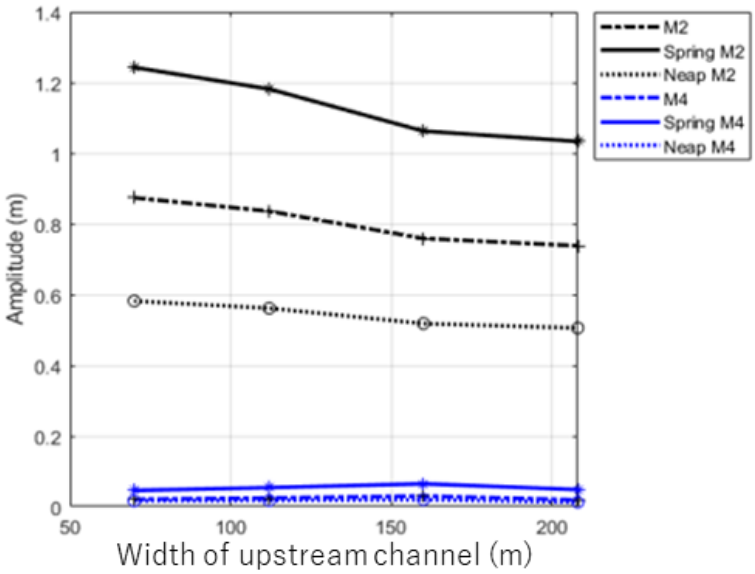

Figure 6. Variation of M2 and M4 amplitude to the width of upstream channel.

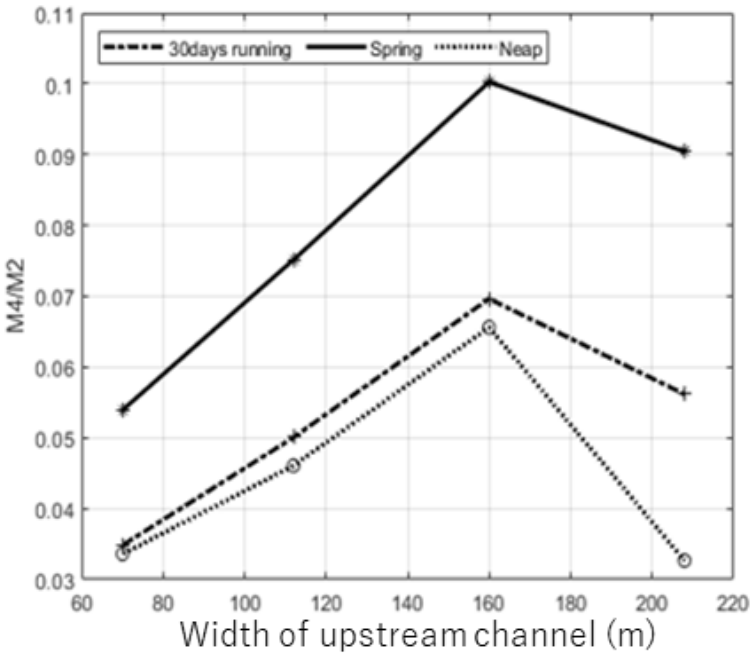

Figure 7. Variation ratio of M4 and M2 to the width of upstream channel.

DOI: https://doi.org/10.17509/ijost.v7i2
p- ISSN 2528-1410 e- ISSN 2527-8045

6. CONCLUSION

Using numerical experiments by variating the width of the upstream channel of the junction, this study shows the effect of the upstream channel width variation on tidal distortion and explains the mechanism behind it. We found that the nonlinearity increased for the width of the upstream channel was less than twice that of the downstream channel, while the falling nonlinearity for the width of the upstream channel was more than double that of the downstream channel.

The increasing nonlinearity was caused by the convergence of tides in the junction. While at the wider junction, the river runoff plays a significant role by damping both M2 and M4, which results in a decrease in tidal nonlinearity. This study limited the investigation of the role of the upstream channel width on water elevation in junctions. Moreover, the model is highly simplified by neglecting the depth variation, real channel length variation, and complexity of the topographical settings. Therefore, a sensitivity analysis that considers these variables should be conducted in the future.

7. ACKNOWLEDGMENT

The author gratefully acknowledges the financial support provided by the Japanese Government (MEXT) scholarship program for his Ph.D. studies at Hiroshima University. We thank the students who participated in the study for their assistance concerning data collection.

8. AUTHORS' NOTE

The authors declare no conflicts of interest regarding the publication of this article. The authors confirm that the paper is free of plagiarism.

9. REFERENCES

Amin, M. H., Sajak, A. A. B., Jaafar, J., Husin, H. S., and Mohamad, S. (2021). Real time water quality monitoring system for smart city in Malaysia. *ASEAN Journal of Science and Engineering*, *2*(1), 47–64.

Arif, N., Danoedoro, P., and Mulabbi, A. (2020). Erosion prediction model using fractional vegetation. *Indonesian Journal of Science and Technology*, *5*(1), 125–132.

Bilskie, M. V., Bacopoulos, P., and Hagen, S. C. (2019). Astronomic tides and nonlinear tidal dispersion for a tropical coastal estuary with engineered features (causeways): Indian River lagoon system. *Estuarine, Coastal and Shelf Science*, *216*, 54–70.

Buschman, F. A., Hoitink, A. J. F., Van Der Vegt, M., and Hoekstra, P. (2010). Subtidal flow division at a shallow tidal junction. *Water Resources Research*, *46*(12), 1–12.

Cai, H., Toffolon, M., Savenije, H. H. G., Yang, Q., and Garel, E. (2018). Frictional interactions between tidal constituents in tide-dominated estuaries. *Ocean Science*, *14*(4), 769–782.

Danial, M. M., Kawanisi, K., and Al Sawaf, M. B. (2019). Characteristics of tidal discharge and phase difference at a tidal channel junction investigated using the fluvial acoustic tomography system. *Water (Switzerland)*, *11*(4), 1-21.

Guo, L., Wegen, M. van der, Jay, D. A., Matte, P., Wang, Z. B., Roelvink, D., and He, Q. (2015). River-tide dynamics: Exploration of nonstationary and nonlinear tidal behavior in the Yangtze River estuary. *Journal of Geophysical Research C: Oceans*, *120*, 3499–3521.

Hoitink, A. J. F., Hoekstra, P., and Van Maren, D. S. (2003). Flow asymmetry associated with astronomical tides: Implications for the residual transport of sediment. *Journal of Geophysical Research C: Oceans*, *108*(10), 1-8.

Horrevoets, A. C., Savenije, H. H. G., Schuurman, J. N., and Graas, S. (2004). The influence of river discharge on tidal damping in alluvial estuaries. *Journal of Hydrology*, *294*(4), 213–228.

Iwantoro, A. P., van der Vegt, M., and Kleinhans, M. G. (2022). Stability and asymmetry of tide‐influenced river bifurcations. *Journal of Geophysical Research: Earth Surface*, *127*(6), 1-24.

Iwantoro, Arya P., Van Der Vegt, M., and Kleinhans, M. G. (2020). Morphological evolution of bifurcations in tide-influenced deltas. *Earth Surface Dynamics*, *8*(2), 413–429.

Khadami, F., Kawanisi, K., Al Sawaf, M. B., Gusti, G. N. N., and Xiao, C. (2022). Spatiotemporal response of currents and mixing to the interaction of tides and river runoff in a mesotidal estuary. *Ocean Science Journal*, *57*(0123456789), 37–51.

Khadami, F., Kawanisi, K., and Tarya, A. (2020). Tidal asymmetry in two-inlet lagoon: a case study on Segara Anakan Lagoon, Central Java, Indonesia. *Journal of Japan Society of Civil Engineers, Ser. B1 (Hydraulic Engineering)*, *76*(2), 1411-1416.

Kukulka, T., and Jay, D. A. (2003). Impacts of Columbia River discharge on salmonid habitat: 1. a nonstationary fluvial tide model. *Journal of Geophysical Research: Oceans*, *108*(9), 1-20.

Lu, S., Tong, C., Lee, D. Y., Zheng, J., Shen, J., Zhang, W., and Yan, Y. (2015). Propagation of tidal waves up in Y angtze E stuary during the dry season. *Journal of Geophysical Research: Oceans*, *120*(9), 6445-6473.

MacMahan, J., van de Kreeke, J., Reniers, A., Elgar, S., Raubenheimer, B., Thornton, E., Brown, J. (2014). Fortnightly tides and subtidal motions in a choked inlet. *Estuarine, Coastal and Shelf Science*, *150*(PB), 325–331.

Matte, P., Secretan, Y., and Morin, J. (2019). Drivers of residual and tidal flow variability in the St. Lawrence fluvial estuary: Influence on tidal wave propagation. *Continental Shelf Research*, *174*(2018), 158–173.

Pareta, K., and Pareta, U. (2017). Geomorphological analysis and hydrological potential zone of Baira River Watershed, Churah in Chamba district of Himachal Pradesh, India. *Indonesian Journal of Science and Technology*, *2*(1), 26–49.

Pawlowicz, R., Pawlowicz, R., Beardsley, R. C., Beardsley, R., Lentz, S., and Lentz, S. (2002). Classical tidal harmonic analysis including error estimates in MATLAB using T_TIDE. *Computers and Geosciences*, *28*(8), 929–937.

Sassi, M. G., and Hoitink, A. J. F. (2013). River flow controls on tides and tide-mean water level profiles in a tidal freshwater river. *Journal of Geophysical Research: Oceans*, *118*(9), 4139–4151.

Sassi, M. G., Hoitink, A. J. F., Vermeulen, B., and Hidayat, H. (2013). Sediment discharge

DOI: https://doi.org/10.17509/ijost.v7i2
p- ISSN 2528-1410 e- ISSN 2527-8045

division at two tidally influenced river bifurcations. *Water Resources Research*, *49*(4), 2119–2134.

Savenije, H. H. G., Toffolon, M., Haas, J., and Veling, E. J. M. (2008). Analytical description of tidal dynamics in convergent estuaries. *Journal of Geophysical Research: Oceans*, *113*(10), 1–18.

Wagner, W., and Mohrig, D. (2019). Flow and sediment flux asymmetry in a branching channel delta. *Water Resources Research*, *55*(11), 9563–9577.

Wu, Y., Hannah, C., Matte, P., O'Flaherty-Sproul, M., Mo, R., Wang, X., and MacAulay, P. (2022). Tidal propagation in the Lower Fraser River, British Columbia, Canada. *Estuarine, Coastal and Shelf Science*, *264*(2021), 107695.

Xiao, C., Kawanisi, K., and Al Sawaf, M. B. (2020). Suspended particulate matter concentration in response to tidal hydrodynamics in a long mesotidal floodway. *Estuarine, Coastal and Shelf Science*, *233*(2019), 106525.

Xiao, C., Kawanisi, K., Torigoe, R., and Al Sawaf, M. B. (2021). Mapping tidal current and salinity at a shallow tidal channel junction using the fluvial acoustic tomography system. *Estuarine, Coastal and Shelf Science*, *258*, 107440.

DOI: https://doi.org/10.17509/ijost.v7i2
p- ISSN 2528-1410 e- ISSN 2527-8045